Mechanism and Machine Theory 200 (2024) 105720

Contents lists available at ScienceDirect

Mechanism and Machine Theory

journal homepage: www.elsevier.com/locate/mechmt

Research paper

Dynamic model of single-DOF spherical mechanisms based on instantaneous pole axes and Eksergian's equation

Raffaele Di Gregorio

Department of Engineering - University of Ferrara, Via Saragat n. 1, 44122, Ferrara (FE), Italy

ARTICLE INFO

Keywords:
Dynamics
Spherical mechanisms
Instantaneous pole axis
Velocity Coefficients

ABSTRACT

Instantaneous pole axes (IPAs) fully describe instantaneous kinematics of spherical mechanisms. In single-degree-of-freedom (single-DOF) mechanisms, IPAs' locations uniquely depend on the mechanism configuration. Such a property allows the deduction of instantaneous-motion characteristics by means of analytic techniques based on geometric features of the mechanism configuration. Moreover, these geometric/analytic approaches are extendable to mechanism's static analyses since the virtual work principle relates mechanism's statics to its instantaneous kinematics. Analytic approaches based on geometric reasoning are of interest in mechanism design and their further extension to dynamic analyses is appealing in that context. This work proposes a possible extension of IPA-based techniques to dynamic analyses of single-DOF spherical mechanisms by using Eksergian's equation. A novel general dynamic model for single-DOF spherical mechanisms is proposed, which is based on IPAs' locations. Then, the effectiveness of the proposed model is applied to a relevant single-DOF spherical mechanism.

1. Introduction

Spherical mechanisms are mechanisms where all the links share a point (spherical motion center), which is fixed in the frame [1]. Such a constraint makes all the links change only their orientation during motion by performing only rotations around axes (pole axes) passing through the spherical motion center. Orientating a rigid body is a motion task that occurs in many applications (e.g., robotic wrists [2-4], prostheses replacing some diathrodial joints [5-8], pointing systems [9-12], etc.), which justify the ample literature addressing the kinematics and dynamics problems involved in spherical mechanisms' design [1,10-20].

Instantaneous kinematics of spherical mechanisms is fully described by the directions of the instantaneous-pole-axes (IPAs) of the relative motions between link couples [21]. In single-DOF spherical mechanisms, such directions depend only on the mechanism configuration and analytic techniques that determine these directions by using only mechanism configuration's data have been proposed in the literature (see, for instance, [22,23]). In particular, the ratios between the rates of two motion variables (e.g., joint rates), named velocity coefficients (VCs), only depend on the generalized coordinate, say q, of the single-DOF mechanism [24] and can be explicitly expressed as functions of IPAs' directions [25].

VCs enter both in statics and dynamics of single-DOF mechanisms [24]. Indeed, the dynamic model of a single-DOF mechanism is buildable by means of Eksergian's equation [26,27]. In so doing, the resulting model directly relates the input generalized torque, which the unique actuator applies, to the generalized coordinate, q, and its time derivatives (i.e., to the resulting motion of the mechanism) thus retaining only the pieces of information necessary to control the mechanism. Such a model involves only the VCs

E-mail address: raffaele.digregorio@unife.it.

https://doi.org/10.1016/j.mechmachtheory.2024.105720
Received 22 April 2024; Received in revised form 16 June 2024; Accepted 16 June 2024
Available online 24 June 2024

Nomenclature

DOF	degree of freedom
RH	reference hemisphere
SMC	spherical motion center
US	unit sphere
VC	velocity coefficient
AC	derivative of a VC with respect to the generalized coordinate, also named *acceleration coefficient*
IPA_{ji}	instantaneous pole axis of the relative motion of link j with respect to link i (Fig. 1)
P_{ji}	intersection point of IPA_{ji} with the RH (Fig. 1)
$\mathbf{u}_{ji}$	unit vector parallel to IPA_{ji} that point toward P_{ji} (Fig. 1)
$\omega_{ji}\mathbf{u}_{ji}$	$(=\boldsymbol{\omega}_{ji})$ angular velocity of the relative motion of link j with respect to link i (Fig. 1); ω_{ji} is its signed magnitude
$Ox_jy_jz_j$	Cartesian reference, fixed to link *j*, that has the origin, O, coincident with the SMC and the y_jz_j-coordinate plane coincident with the plane, which contains the great circle arc of US that locates the pose of link *j* on the US (see Fig. 3)
${}^{j}\mathbf{R}_{f}$	rotation matrix that transforms vector components measured in $Ox_fy_fz_f$, fixed to link *f*, into the components of the same vector measured in $Ox_jy_jz_j$, fixed to link *j* (Fig. 3)
q	generalized coordinate
Q_j	contribution to the *generalized force*, Q $(=\sum_{j=1,m} Q_j)$, due to all the active loads (forces and moments) applied to the *j*-th link
B	equivalent moment of inertia of a single-DOF mechanism
E	total kinetic energy of a mechanism
$\mathbf{I}_{O,j}$	inertia tensor of link *j* about point O
$I_{(O,\mathbf{u}_{jf})}$	$(=\mathbf{u}_{jf}\cdot(\mathbf{I}_{O,j}\mathbf{u}_{jf}))$ inertia moment of link *j* with respect to the line IPA_{jf}, also denoted $(O,\mathbf{u}_{jf})$
${}^{j}(\cdot)$	the rear superscript *j* on a vector (an inertia tensor) symbol, $(\cdot)$, indicates that the components (the entries) of the vector (of the inertia tensor) are measured in the Cartesian reference fixed to link *j*

over, of course, the mass distribution data of the links and the active forces applied to them.

By combining the fact that VCs are expressible through IPAs' directions and that Eksergian's equation provides a VC-based dynamic model, this work proposes a novel general dynamic model for single-DOF spherical mechanisms, which extends the above-mentioned analytic approaches based on geometric reasoning to the dynamic analysis of these mechanisms. Also, in this paper, the procedures that use the novel model for the solution of the direct and the inverse dynamic problems are presented and, then, are applied to a relevant case study to better illustrate them. These results provide new tools for designing single-DOF spherical mechanisms by taking into account requirements on their dynamic performances. Since these tools are based on geometric reasoning, they are able to evaluate the effects of geometric changes onto the mechanism behavior, which is exactly what designers need.

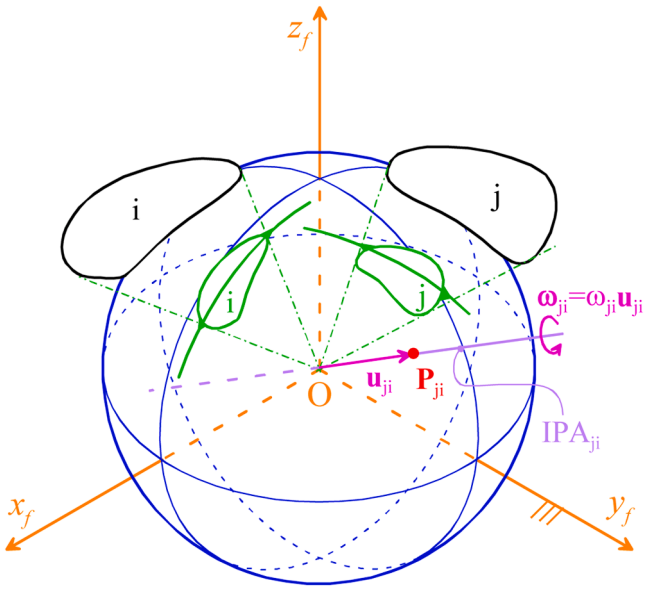

Fig. 1. Links *j* and *i* projected from the spherical motion center (SMC), point O, onto a sphere (unit sphere (US)) with unitary radius and center at O.

This paper is organized as follows. Section 2 recalls the necessary background materials, deduces the novel dynamic model, and presents the algorithms to implement the solution of the direct and the inverse dynamic problems by means of the new model. Section 3 applies the proposed algorithms to a relevant single-DOF spherical mechanism. Section 4 discusses the results and Section 5 draws the conclusions.

2. Materials and methods

Kinematics of spherical mechanisms can be studied [22] by projecting (see Fig. 1) the links from the spherical motion center (SMC), point O in Fig. 1, onto a sphere (unit sphere (US)) with unitary radius and center at the projection center. Doing so, the links become spherical laminae that slide on the US; also, the mechanism kinematics can be studied by analyzing how these laminae move on the US, which is the same as studying the motion of great circle arcs, one for each link, fixed to those spherical laminae. Any line passing through the SMC may become a particular IPA during the mechanism motion. Such lines intersect the US at two diametrically opposite points; consequently, in order to state a one-to-one correspondence between points on the US and IPAs, it is necessary to choose which one out of these two intersections must be selected. This choice can be done by cutting the US into two hemispheres with a cut along a great circle and by choosing which hemisphere is the reference one [22] for the selection of the intersection. On the so-chosen reference hemisphere (RH), the minimum distance between two points is the length of the great circle arc joining the two points, each point uniquely individuates a possible IPA and can be located by its coordinates in a Cartesian reference (reference $Ox_fy_fz_f$ in Fig. 1), fixed to the mechanism frame (link *f*), with origin at the SMC. Such coordinates are, at the same time, the components, in the same Cartesian reference, of a unit vector parallel to the IPA.

Hereafter, with reference to two links (see Fig. 1), say links *i* and *j*, IPA_{ji}, P_{ji}, and $\mathbf{u}_{ji}$ will denote the IPA of the relative motion of link *j* with respect to link *i* (hereafter, named *ji* relative motion), the intersection point of that IPA with the RH, and the unit vector parallel to the same IPA that points toward P_{ji}, respectively. Also, ω_{ji} will denote the signed magnitude of the angular velocity, $\boldsymbol{\omega}_{ji}$, of the *ji* relative motion, with the sign of ω_{ji} defined so that $\boldsymbol{\omega}_{ji}=\omega_{ji}\mathbf{u}_{ji}$. These notations together with the relative motion theorems [28] yield the following relationships:

$$\mathrm{IPA}_{ji}=\mathrm{IPA}_{ij};\mathrm{P}_{ji}=\mathrm{P}_{ij};\mathbf{u}_{ji}=\mathbf{u}_{ij};\omega_{ji}=-\omega_{ij} \tag{1}$$

The Aronhold-Kennedy (A-K) theorem for spherical motion [1] can be enunciated as follows: "*If the three links i, j, and k perform an instantaneous spherical motion with the same SMC, then P_{ji}, P_{jk}, and P_{ki} must lie on the same great circle of the US*". The A-K theorem implies the coplanarity of IPA_{ji}, IPA_{jk}, and IPA_{ki}, which analytically is expressible as follows:

$$\mathbf{u}_{ji}\cdot\left(\mathbf{u}_{jk}\times\mathbf{u}_{ki}\right)=0 \tag{2}$$

Also, the A-K theorem allows the determination of IPA_{ji} if there are two couples of known IPAs that share a common index in the front subscript whose elimination leaves, in both the couples, the indices *j* and *i*. Indeed (see Fig. 2), if IPA_{jk}, IPA_{ik}, IPA_{jr}, and IPA_{ir}, are known (i.e., $\mathbf{u}_{jk}$, $\mathbf{u}_{ik}$, $\mathbf{u}_{jr}$, and $\mathbf{u}_{ir}$ are known), the A-K theorem implies that IPA_{ji} must lie both on the plane located by IPA_{jk} and IPA_{ik} (i.e., the one perpendicular to $\mathbf{u}_{jk}\times\mathbf{u}_{ki}$ and passing through the SMC) and on the plane located by IPA_{jr} and IPA_{ir} (i.e., the one perpendicular to $\mathbf{u}_{jr}\times\mathbf{u}_{ri}$ and passing through the SMC); as a consequence, IPA_{ji} must be the intersection line of those two planes, that is, it is the line passing through the SMC whose direction is immediately computable with the following explicit formula:

$$\mathbf{u}_{ji}=\frac{\left(\mathbf{u}_{jk}\times\mathbf{u}_{ki}\right)\times\left(\mathbf{u}_{jr}\times\mathbf{u}_{ri}\right)}{\|\left(\mathbf{u}_{jk}\times\mathbf{u}_{ki}\right)\times\left(\mathbf{u}_{jr}\times\mathbf{u}_{ri}\right)\|} \tag{3}$$

Moreover, for the same system of three links, the A-K theorem refers to, the relative motion theorems [28] relate their relative angular velocities (i.e., $\boldsymbol{\omega}_{ji}$, $\boldsymbol{\omega}_{jk}$, and $\boldsymbol{\omega}_{ki}$) through the relationship

$$\omega_{ji}\mathbf{u}_{ji}=\omega_{jk}\mathbf{u}_{jk}+\omega_{ki}\mathbf{u}_{ki} \tag{4}$$

whose dot product by $\mathbf{u}_{ji}\times\left(\mathbf{u}_{jk}\times\mathbf{u}_{ki}\right)$ yields

$$\omega_{jk}\left\{\mathbf{u}_{jk}\cdot\left[\mathbf{u}_{ji}\times\left(\mathbf{u}_{jk}\times\mathbf{u}_{ki}\right)\right]\right\}=\omega_{ik}\left\{\mathbf{u}_{ki}\cdot\left[\mathbf{u}_{ji}\times\left(\mathbf{u}_{jk}\times\mathbf{u}_{ki}\right)\right]\right\}\Rightarrow\frac{\omega_{jk}}{\omega_{ik}}=\frac{\mathbf{u}_{ki}\cdot\left[\mathbf{u}_{ji}\times\left(\mathbf{u}_{jk}\times\mathbf{u}_{ki}\right)\right]}{\mathbf{u}_{jk}\cdot\left[\mathbf{u}_{ji}\times\left(\mathbf{u}_{jk}\times\mathbf{u}_{ki}\right)\right]}\equiv\frac{\left(\mathbf{u}_{jk}\times\mathbf{u}_{ki}\right)\cdot\left(\mathbf{u}_{ji}\times\mathbf{u}_{ki}\right)}{\left(\mathbf{u}_{jk}\times\mathbf{u}_{ki}\right)\cdot\left(\mathbf{u}_{ji}\times\mathbf{u}_{jk}\right)} \tag{5}$$

Eq. (5) provides the explicit expression of any VC as function of the IPA directions in a system of three links, which could also be a sub-system of any spherical mechanism. This type of VCs are characterized by the fact that the two motion-variable rates[1] they relate share one index in the front subscript (in Eq. (5), the shared index is *k*). Over this case, there is only the other case where the VC is the ratio of two motion-variable rates that do not share any index in their front subscripts. This other case refers to a system of four links,

[1] In spherical mechanisms, the motion-variable rates are always signed magnitudes of angular velocities since only instantaneous rotations are possible.

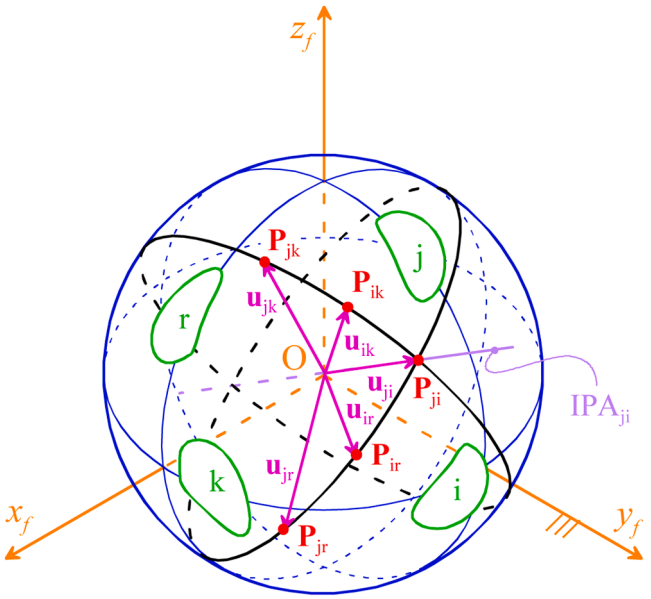

Fig. 2. Geometric construction, based on the A-K theorem, for the determination of IPA_{ji} starting from assigned values of $\mathbf{u}_{jk}$, $\mathbf{u}_{ik}$, $\mathbf{u}_{jr}$, and $\mathbf{u}_{ir}$ in a four-link system constituted of links *i, j, k*, and *r*.

say links *i, j, k*, and *l*. In a system of four links, six relative motions and as many IPAs are definable,[2] that is, the relative motions *ji, jk, jl, ki, kl*, and *il*, and the relative motion theorems [28] state the following relationships among them

$$\omega_{ji}\mathbf{u}_{ji} = \omega_{jk}\mathbf{u}_{jk} + \omega_{ki}\mathbf{u}_{ki} \tag{6a}$$

$$\omega_{jl}\mathbf{u}_{jl} = \omega_{jk}\mathbf{u}_{jk} + \omega_{kl}\mathbf{u}_{kl} \tag{6b}$$

$$\omega_{il}\mathbf{u}_{il} = -\omega_{ki}\mathbf{u}_{ki} + \omega_{kl}\mathbf{u}_{kl} \tag{6c}$$

The sum of Eqs. (6a) and (6c) yields

$$\omega_{ji}\mathbf{u}_{ji} + \omega_{il}\mathbf{u}_{il} = \omega_{jk}\mathbf{u}_{jk} + \omega_{kl}\mathbf{u}_{kl} \tag{7}$$

whose dot product by $(\mathbf{u}_{il} \times \mathbf{u}_{jk})$ gives

$$\omega_{ji}\mathbf{u}_{ji} \cdot (\mathbf{u}_{il} \times \mathbf{u}_{jk}) = \omega_{kl}\mathbf{u}_{kl} \cdot (\mathbf{u}_{il} \times \mathbf{u}_{jk}) \Rightarrow \frac{\omega_{ji}}{\omega_{kl}} = \frac{\mathbf{u}_{kl} \cdot (\mathbf{u}_{il} \times \mathbf{u}_{jk})}{\mathbf{u}_{ji} \cdot (\mathbf{u}_{il} \times \mathbf{u}_{jk})} \tag{8}$$

Eq. (8) provides the explicit expression of any VC as function of the IPA directions in a system of four links, that is, in the case where the VC is the ratio between two motion-variable rates that do not share any index in the front subscript. Eqs. (5) and (8) cover all the possible cases.

The effective use of formulas (5) and (8) is intimately related to the availability of exhaustive algorithms that compute the IPA directions starting from the value of the generalized coordinate, *q*, of the single-DOF spherical mechanism. This author proposed one of such algorithms in [22], which is summarizable as follows. The IPAs can be collected into two sets: the primary IPAs, which are the one determinable through a simple inspection of the mechanism configuration, and the secondary IPAs, which are computable by using as starting data the directions of the primary IPAs. The primary IPAs refer to the relative motions between links joined by a kinematic pair. In spherical mechanisms, the kinematic pairs are only of three types: (i) revolute (R) pair, whose IPA is the R-pair axis, (ii) rolling contact (C_r), whose IPA is the contact line, and (iii) slipping contact (C_s), whose IPA lies on the plane passing through the contact line and perpendicular to the surfaces that touch each other to form the C_s. From an analytic point of view, the directions of the primary IPAs as a function of the generalized coordinate are immediately known after having solved the system of constraint equations of the mechanism; whereas, from a geometric point of view, a simple inspection of a 3D view of the mechanism configuration is sufficient to locate them. Once the directions of the primary IPAs have been determined, the secondary IPAs are computable in general by repeatedly applying the A-K theorem [22], that is, by repeatedly applying Eq. (3), for computing a suitable sequence of secondary IPAs;

[2] The *ji* and the *ij* relative (spherical) motions are considered the same relative motion since the IPA is the same and $\omega_{ji} = -\omega_{ij}$. In a set of *n* links, $n(n–1)/2$ relative motions are definable and, in the case of spherical motion, as many IPAs, but only $(n–1)$ are independent since all the data of the remaining relative motions can be computed through the relative motion theorems [28].

in some mechanisms, named "indeterminate mechanisms", this simple procedure becomes a bit more complex as detailed in [22]. Anyway, all the possible cases can be included in a general algorithm applicable to any spherical mechanism [22]. The conclusion is that VCs are indeed an effective tool when used in solving kinematics and dynamics problems of spherical mechanisms.

2.1. Dynamic model

Eksergian's equation [24,26,27] holds for single-DOF mechanisms with time-independent[3] (scleronomic) holonomic constraints, that is, for the vast majority of single-DOF mechanisms. Hereafter, for the sake of brevity, if not differently specified, the term "mechanism" will refer to a "mechanism with time-independent holonomic constraints".

The general expression of Eksergian's equation (see Appendix A) for a single-DOF mechanism with m links can be written as follows

$$\sum_{j=1,m} Q_j = B\ddot{q} + \frac{1}{2}\frac{dB}{dq}\dot{q}^2 \tag{9}$$

where q is the *generalized coordinate*, Q_j is the contribution to the *generalized force*, Q $\left(=\sum_{j=1,m} Q_j\right)$, due to all the active loads (forces and moments) applied to the j-th link, and B is the *equivalent moment of inertia* of the mechanism. B depends only on q and is related to the total kinetic energy, E, of the mechanism by the relationship

$$B = \frac{2E}{\dot{q}^2} \tag{10}$$

2.1.1. Deduction of the model

In a spherical mechanism, any system of forces applied to the j-th link can be reduced to a resultant force, $\mathbf{F}_j$, applied to the SMC and a resultant moment, $\mathbf{M}_{O,j}$, about the SMC with

$$\mathbf{F}_j = \sum_{k=1,n_j} \mathbf{F}_{j,k}; \qquad \mathbf{M}_{Oj} = \sum_{k=1,n_j} \left(A_{j,k} - O\right) \times \mathbf{F}_{j,k} = \sum_{k=1,n_j} \left(A_{j,k} - O\right) \times \left(F_{j,k}\mathbf{v}_{j,k}\right); \tag{11}$$

where n_j is the number of forces applied to link j; $\mathbf{F}_{j,k}$ is the k-th force, for k=1, …, n_j, applied to link j with its direction given by unit vector $\mathbf{v}_{j,k}$ and with its signed magnitude given by $F_{j,k}$, defined so that relationship $\mathbf{F}_{j,k} = F_{j,k}\mathbf{v}_{j,k}$ holds; and[4] $A_{j,k}$ is the position vector of the application point $\mathrm{A}_{j,k}$ of $\mathbf{F}_{j,k}$ measured in the Cartesian reference $Ox_fy_fz_f$ fixed to mechanism's frame (see Figs. 1 and 2), from now on named link f. Since the reduction point (i.e., the SMC) is at rest, the virtual work principle [29] allows the analytic computation of the contribution, Q_j, to the generalized force of all the loads applied to the j-th link of a single-DOF spherical mechanism as follows

$$\left[\delta L_j = \mathbf{M}_{Oj}\cdot\mathbf{u}_{jf}\delta\theta_{jf} = \mathbf{M}_{Oj}\cdot\mathbf{u}_{jf}\left(\frac{\omega_{jf}}{\dot{q}}\right)\delta q = \quad = \left[\sum_{k=1,n_j} F_{j,k}\left(A_{j,k}-O\right)\times\mathbf{v}_{j,k}\right]\cdot\mathbf{u}_{jf}\left(\frac{\omega_{jf}}{\dot{q}}\right)\delta q = Q_j\delta q\right\rangle \Rightarrow Q_j(q)$$

$$= \left(\frac{\omega_{jf}}{\dot{q}}\right)\sum_{k=1,n_j} F_{j,k}\left\{\left[\left(A_{j,k}-O\right)\times\mathbf{v}_{j,k}\right]\cdot\mathbf{u}_{jf}\right\} \tag{12}$$

It is worth noting that formula (12) is the product of the velocity coefficient $\left(\omega_{jf}/\dot{q}\right)$, which is expressible as a function of IPA directions through Eqs. (5) or (8), by a summation that contains only position vectors, unit vectors parallel to either forces or to IPA_{jf}, and signed magnitudes of forces, which confirms that Q_j uniquely depends on q.

Also, the kinetic energy of link j, which performs a spherical motion with point O as SMC, measured from link f (i.e., the frame), is expressible in explicit form as follows

$$E_j = \frac{1}{2}\omega_{jf}^2\mathbf{u}_{jf}\cdot\left(\mathbf{I}_{Oj}\mathbf{u}_{jf}\right) = \frac{1}{2}I_{\left(O,\mathbf{u}_{jf}\right)}\omega_{jf}^2 \tag{13}$$

where $\left(O,\mathbf{u}_{jf}\right)$ denotes the instantaneous pole axis IPA_{jf} of the jf relative motion; $\boldsymbol{\omega}_{jf} = \omega_{jf}\mathbf{u}_{jf}$ is the angular velocity of the same relative motion; $\mathbf{I}_{O,j}$ is the inertia tensor of link j about point O and $I_{\left(O,\mathbf{u}_{jf}\right)} = \mathbf{u}_{jf}\cdot\left(\mathbf{I}_{Oj}\mathbf{u}_{jf}\right)$ is the inertia moment of link j with respect to the line $\left(O,\mathbf{u}_{jf}\right)$ (i.e., the IPA_{jf}). Eq. (13) yields the following explicit expression of the total kinetic energy of the mechanism measured from its frame (link f)

[3] It is worth noting that only mechanisms with mobile frames have time-dependent constraints.

[4] Hereafter, a point will be denoted with a capital letter in plain text (e.g., P), and the same letter in italic (e.g., P) will denote the position vector of that point measured in the Cartesian reference $Ox_fy_fz_f$, fixed to the frame (see Figs. 1 and 2).

$$E=\sum_{j=1,m}E_j=\frac{1}{2}\dot{q}^2\sum_{j=1,m}\left(\frac{\omega_{jf}}{\dot{q}}\right)^2\mathbf{u}_{jf}\cdot\left(\mathbf{I}_{O,j}\mathbf{u}_{jf}\right)=\frac{1}{2}\dot{q}^2\sum_{j=1,m}I_{(O,\mathbf{u}_{jf})}\left(\frac{\omega_{jf}}{\dot{q}}\right)^2=\frac{1}{2}B\dot{q}^2 \tag{14}$$

which, when introduced into Eq. (10), provides, for B, the explicit formula

$$B(q)=\sum_{j=1,m}\left(\frac{\omega_{jf}}{\dot{q}}\right)^2\mathbf{u}_{jf}\cdot\left(\mathbf{I}_{O,j}\mathbf{u}_{jf}\right)=\sum_{j=1,m}\left(\frac{\omega_{jf}}{\dot{q}}\right)^2{}^f\mathbf{u}_{jf}^{Tj}\mathbf{R}_f^{Tj}\mathbf{I}_{O,j}{}^j\mathbf{R}_f{}^f\mathbf{u}_{jf} \tag{15}$$

where the index reported as rear superscript on a vector (an inertia tensor) symbol indicates that the components (the entries) of the vector (of the inertia tensor) are measured in the Cartesian reference fixed to the link with that index; also, ${}^j\mathbf{R}_f$ denotes the rotation matrix that transforms vector components measured in the reference system $Ox_fy_fz_f$ (see Fig. 3), fixed to link f, into the components of the same vector measured in the reference system fixed to link j (system $Ox_jy_jz_j$ in Fig. 3). Hereafter, with reference to Fig. 3, the orientation of link j with respect to link f will be identified by the pose on the US of a great circle arc, fixed to link j, with α_j denoting the central angle subtended by the arc, by introducing a Cartesian reference $Ox_jy_jz_j$, fixed to link j, with origin at the SMC (i.e., point O in Fig. 3) and y_jz_j-coordinate plane containing the arc and the SMC and by giving the rotation matrix ${}^f\mathbf{R}_j(={}^j\mathbf{R}_f^T)$.

Eq. (15), over the mass distribution data of the links, contains VCs and $\mathbf{u}_{jf}$, that is, parameters related to the IPA directions, which confirms that B uniquely depends on q. The introduction of Eqs. (12) and (15) into Eq. (9) yields

$$\sum_{j=1,m}\left(\frac{\omega_{jf}}{\dot{q}}\right)\sum_{k=1,n_j}F_{j,k}\mathbf{u}_{jf}\cdot\left[\left(A_{j,k}-O\right)\times\mathbf{v}_{j,k}\right]=\ddot{q}\sum_{j=1,m}\left(\frac{\omega_{jf}}{\dot{q}}\right)^2\mathbf{u}_{jf}\cdot\left(\mathbf{I}_{O,j}\mathbf{u}_{jf}\right)+\frac{1}{2}\dot{q}^2\frac{d}{dq}\left(\sum_{j=1,m}\left(\frac{\omega_{jf}}{\dot{q}}\right)^2\mathbf{u}_{jf}\cdot\left(\mathbf{I}_{O,j}\mathbf{u}_{jf}\right)\right) \tag{16}$$

which can be expanded as follows

$$\begin{aligned}\sum_{j=1,m}\left(\frac{\omega_{jf}}{\dot{q}}\right)\sum_{k=1,n_j}F_{j,k}\mathbf{u}_{jf}\cdot\left[\left(A_{j,k}-O\right)\times\mathbf{v}_{j,k}\right]&=\ddot{q}\sum_{j=1,m}\left(\frac{\omega_{jf}}{\dot{q}}\right)^2{}^f\mathbf{u}_{jf}^{Tj}\mathbf{R}_f^{Tj}\mathbf{I}_{O,j}{}^j\mathbf{R}_f{}^f\mathbf{u}_{jf}+\\&+\frac{1}{2}\dot{q}^2\sum_{j=1,m}\left(\frac{\omega_{jf}}{\dot{q}}\right)\left\{2{}^f\mathbf{u}_{jf}^{Tj}\mathbf{R}_f^{Tj}\mathbf{I}_{O,j}{}^j\mathbf{R}_f{}^f\mathbf{u}_{jf}\frac{d}{dq}\left(\frac{\omega_{jf}}{\dot{q}}\right)\right.\\&\left.+\left(\frac{\omega_{jf}}{\dot{q}}\right)\left[\frac{d\left({}^j\mathbf{R}_f{}^f\mathbf{u}_{jf}\right)^T}{dq}{}^j\mathbf{I}_{O,j}{}^j\mathbf{R}_f{}^f\mathbf{u}_{jf}+{}^f\mathbf{u}_{jf}^{Tj}\mathbf{R}_f^{Tj}\mathbf{I}_{O,j}\frac{d\left({}^j\mathbf{R}_f{}^f\mathbf{u}_{jf}\right)}{dq}\right]\right\}\end{aligned} \tag{17}$$

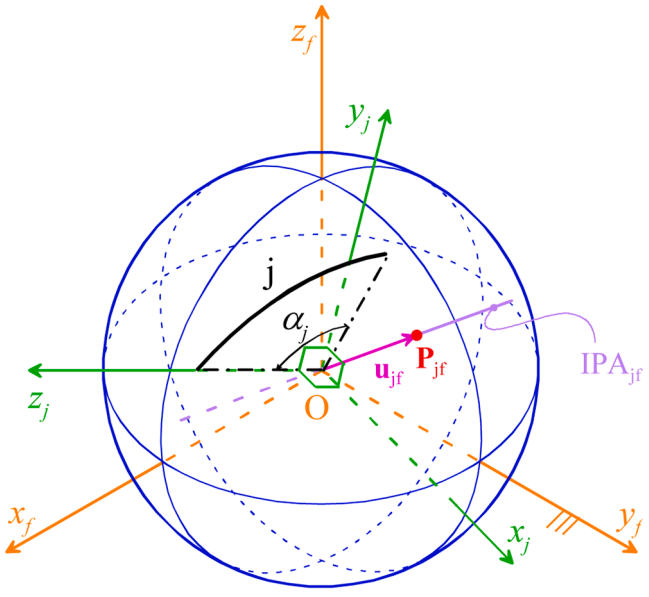

Fig. 3. A great circle arc of the US that is fixed to link j: α_j is the central angle subtended by the arc, $Ox_jy_jz_j$ is a Cartesian reference, fixed to link j, with origin at the SMC (point O) and y_jz_j-coordinate plane containing the arc and the SMC, $Ox_fy_fz_f$ is a Cartesian reference fixed to mechanism's frame (link f).

where

$$\frac{d\left({}^{j}\mathbf{R}_{f}{}^{f}\mathbf{u}_{jf}\right)}{dq}=\frac{d\left({}^{j}\mathbf{R}_{f}\right)}{dq}{}^{f}\mathbf{u}_{jf}+{}^{j}\mathbf{R}_{f}\frac{d\left({}^{f}\mathbf{u}_{jf}\right)}{dq} \tag{18}$$

and the following relationship has been used

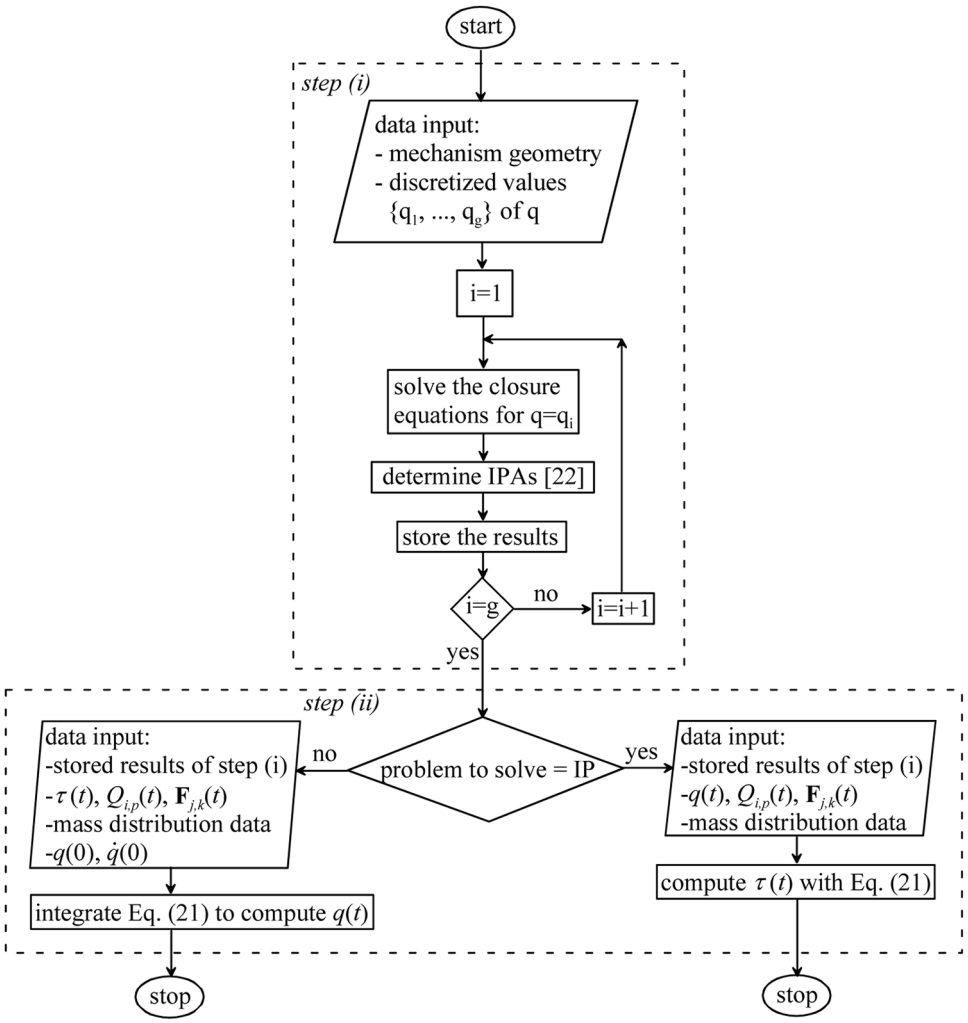

Fig. 4. Flow-chart of the algorithms for the solution of dynamics' problems.

$$\frac{dB}{dq}=\frac{d}{dq}\left(\sum_{j=1,m}\left(\frac{\omega_{jf}}{\dot{q}}\right)^2\mathbf{u}_{jf}\cdot\left(\mathbf{I}_{Oj}\mathbf{u}_{jf}\right)\right)=\left\{2\mathbf{u}_{jf}\cdot\left(\mathbf{I}_{Oj}\mathbf{u}_{jf}\right)\frac{d}{dq}\left(\frac{\omega_{jf}}{\dot{q}}\right)+\left(\frac{\omega_{jf}}{\dot{q}}\right)\left[\frac{d\mathbf{u}_{jf}}{dq}\cdot\left(\mathbf{I}_{Oj}\mathbf{u}_{jf}\right)+\mathbf{u}_{jf}\cdot\left(\frac{d\left(\mathbf{I}_{Oj}\mathbf{u}_{jf}\right)}{dq}\right)\right]\right\}=$$

$$=\sum_{j=1,m}\left(\frac{\omega_{jf}}{\dot{q}}\right)$$

$$=\sum_{j=1,m}\left(\frac{\omega_{jf}}{\dot{q}}\right)\left\{2{}^f\mathbf{u}_{jf}^{Tj}\mathbf{R}_f^{Tj}\mathbf{I}_{Oj}{}^j\mathbf{R}_f{}^f\mathbf{u}_{jf}\frac{d}{dq}\left(\frac{\omega_{jf}}{\dot{q}}\right)+\quad+\left(\frac{\omega_{jf}}{\dot{q}}\right)\left[\frac{d\left({}^j\mathbf{R}_f{}^f\mathbf{u}_{jf}\right)^T}{dq}{}^j\mathbf{I}_{Oj}{}^j\mathbf{R}_f{}^f\mathbf{u}_{jf}+{}^f\mathbf{u}_{jf}^{Tj}\mathbf{R}_f^{Tj}\mathbf{I}_{Oj}\frac{d\left({}^j\mathbf{R}_f{}^f\mathbf{u}_{jf}\right)}{dq}\right]\right\} \tag{19}$$

Eq. (17) where all the VCs are expressed through Eqs. (5) or (8) is the sought-after model. Such a model, over the load data and the mass distribution data, contains only the IPA directions and their first derivatives with respect to q (i.e., the tangents to the fixed-axode cones) that appear in the VCs' derivatives (usually named *acceleration coefficients* (ACs)).

By choosing link i as input link, the following relationships hold

$$\dot{q}=\omega_{if}\Rightarrow\left(\frac{\omega_{if}}{\dot{q}}\right)=1\Rightarrow Q_i=\sum_{k=1,n_i}F_{i,k}\mathbf{u}_{if}\cdot\left[\left(A_{i,k}-O\right)\times\mathbf{v}_{i,k}\right]=\tau+Q_{i,p}, \tag{20}$$

where $Q_{i,p}$ collects all the terms of the summation that gives Q_i but the one, τ, due to the actuator. The introduction of Eqs. (20) into Eq. (17) transforms the dynamic model as follows:

$$\tau+Q_{i,p}+\sum_{\substack{j=1,m\\ j\neq i}}\left(\frac{\omega_{jf}}{\dot{q}}\right)\sum_{k=1,n_j}F_{j,k}\mathbf{u}_{jf}\cdot\left[\left(A_{j,k}-O\right)\times\mathbf{v}_{j,k}\right]=\ddot{q}\sum_{j=1,m}\left(\frac{\omega_{jf}}{\dot{q}}\right)^2{}^f\mathbf{u}_{jf}^{Tj}\mathbf{R}_f^{Tj}\mathbf{I}_{Oj}{}^j\mathbf{R}_f{}^f\mathbf{u}_{jf}$$

$$+\quad+\frac{1}{2}\dot{q}^2\sum_{j=1,m}\left(\frac{\omega_{jf}}{\dot{q}}\right)\left\{2{}^f\mathbf{u}_{jf}^{Tj}\mathbf{R}_f^{Tj}\mathbf{I}_{Oj}{}^j\mathbf{R}_f{}^f\mathbf{u}_{jf}\frac{d}{dq}\left(\frac{\omega_{jf}}{\dot{q}}\right)+\quad+\left(\frac{\omega_{jf}}{\dot{q}}\right)\left[\frac{d\left({}^j\mathbf{R}_f{}^f\mathbf{u}_{jf}\right)^T}{dq}{}^j\mathbf{I}_{Oj}{}^j\mathbf{R}_f{}^f\mathbf{u}_{jf}+{}^f\mathbf{u}_{jf}^{Tj}\mathbf{R}_f^{Tj}\mathbf{I}_{Oj}\frac{d\left({}^j\mathbf{R}_f{}^f\mathbf{u}_{jf}\right)}{dq}\right]\right\} \tag{21}$$

2.1.2. *Procedures for the solution of dynamics' problems*

The problems of mechanisms' dynamics are mainly two: the direct problem (DP) and the inverse problem (IP). In single-DOF mechanisms, the DP is the determination of the generalized coordinate, $q(t)$, as a function of time, t, once the initial values, $q(0)$ and $\dot{q}(0)$, are assigned together with the time histories of all the active loads applied to the mechanism, included the one, $\tau(t)$, applied by the actuator to the input link, usually named *generalized torque*. Vice versa, the IP is the determination of the time history, $\tau(t)$, of the generalized torque, once the time histories of the generalized coordinate, $q(t)$, and of all the remaining active loads are assigned. Both the problems require the solution of Eq. (21). Nevertheless, in the DP solution, Eq. (21) is a non-linear differential equation (i.e., the DP solution is difficult and, often, requires numerical integrations); whereas, in the IP solution, Eq. (21) is a linear algebraic equation whose solution is straightforward.

The following procedure is implementable to solve Eq. (21) in both the cases (see Fig. 4):

i) the range of variation of q is discretized into a sufficiently-high number, say g, of values $\{q_1, \ldots, q_g\}$ and, for each of such values, the system of closure equations of the mechanism is solved and all the necessary IPA directions are computed through, for instance, the algorithms presented in [22] and stored;
ii) *if* the IP has to be solved, *then*, the known time history $q(t)$ is discretized and, for each discretized value, the active load data together with the stored results of step (i) are introduced into Eq. (21), written by isolating τ on the left-hand side, to immediately compute the corresponding generalized torque value; *else* (the DP has to be solved), the active load data and the stored results of step (i) together with the initial values, $q(0)$ and $\dot{q}(0)$, are used to start an iterative numerical algorithm [30] that integrates Eq. (21) to compute discretized values of the sought-after time history $q(t)$.

3. Results

In this section, the above-deduced dynamic model is built for a spherical four-bar linkage (Fig. 5(a)). Successively, such a model is used to implement the IP solution of a numerical case with the above-proposed procedures and to provide the iterative formula to use for the solution of its DP with the same procedures.

3.1. Dynamic model of a spherical four-bar linkage

Fig. 5(b) shows a spherical four-bar linkage together with the directions of the four primary IPAs (i.e., the unit vectors $\mathbf{u}_{21}$, $\mathbf{u}_{32}$, $\mathbf{u}_{43}$, and $\mathbf{u}_{41}$) and the geometric determination of the directions of the two remaining secondary IPAs (i.e., the unit vectors $\mathbf{u}_{31}$ and $\mathbf{u}_{42}$). With reference to Fig. 5(a), link 1 is the frame (i.e., f=1) and the joint variable θ_{21} is chosen as the generalized coordinate (i.e., q=θ_{21}). Also, with reference to the j-th link, for j=1, …, 4, $\mathbf{i}_j$, $\mathbf{j}_j$, and $\mathbf{k}_j$ will denote the unit vectors of the coordinate axes x_j, y_j and z_j, respectively, of the reference system $Ox_jy_jz_j$ fixed to the generic link j (see Fig. 3). With the notations introduced in Fig. 5, the following relationships hold

$$\mathbf{u}_{41}=\mathbf{k}_1;\qquad \mathbf{u}_{21}=\mathbf{j}_1\sin\alpha_1+\mathbf{k}_1\cos\alpha_1=\mathbf{k}_2;\qquad \mathbf{j}_2=\mathbf{i}_1\sin\theta_{21}+\cos\theta_{21}(\mathbf{k}_1\sin\alpha_1-\mathbf{j}_1\cos\alpha_1) \tag{22a}$$

$$\mathbf{i}_2=\mathbf{j}_2\times\mathbf{k}_2;\qquad \mathbf{u}_{32}=\mathbf{u}_{21}\cos\alpha_2+\mathbf{j}_2\sin\alpha_2=\mathbf{k}_3;\qquad \mathbf{u}_{43}=\mathbf{k}_1\cos\alpha_4+\sin\alpha_4(\mathbf{i}_1\sin\theta_{41}-\mathbf{j}_1\cos\theta_{41})=\mathbf{k}_4 \tag{22b}$$

$$\mathbf{i}_3=\frac{\mathbf{u}_{43}\times\mathbf{u}_{32}}{\sin\alpha_3};\qquad \mathbf{j}_3=\mathbf{k}_3\times\mathbf{i}_3;\qquad \mathbf{i}_4=\frac{\mathbf{u}_{41}\times\mathbf{u}_{43}}{\sin\alpha_4};\qquad \mathbf{j}_4=\mathbf{k}_4\times\mathbf{i}_4; \tag{22c}$$

$${}^2\mathbf{R}_1^T={}^1\mathbf{R}_2=\left[{}^1\mathbf{i}_2\ {}^1\mathbf{j}_2\ {}^1\mathbf{k}_2\right];\qquad {}^3\mathbf{R}_1^T={}^1\mathbf{R}_3=\left[{}^1\mathbf{i}_3\ {}^1\mathbf{j}_3\ {}^1\mathbf{k}_3\right];\qquad {}^4\mathbf{R}_1^T={}^1\mathbf{R}_4=\left[{}^1\mathbf{i}_4\ {}^1\mathbf{j}_4\ {}^1\mathbf{k}_4\right] \tag{22d}$$

$$\mathbf{u}_{31}=\frac{(\mathbf{u}_{41}\times\mathbf{u}_{43})\times(\mathbf{u}_{21}\times\mathbf{u}_{32})}{\|(\mathbf{u}_{41}\times\mathbf{u}_{43})\times(\mathbf{u}_{21}\times\mathbf{u}_{32})\|};\qquad \mathbf{u}_{42}=\frac{(\mathbf{u}_{21}\times\mathbf{u}_{41})\times(\mathbf{u}_{32}\times\mathbf{u}_{43})}{\|(\mathbf{u}_{21}\times\mathbf{u}_{41})\times(\mathbf{u}_{32}\times\mathbf{u}_{43})\|}. \tag{22e}$$

In Eqs. (22), only the joint variable θ_{41} appears over the generalized coordinate θ_{21}. The closure equation that relates these two motion variables is deducible by noting that (Fig. 5):

$$\mathbf{u}_{43}\cdot\mathbf{u}_{32}=\cos\alpha_3 \tag{23}$$

which, by introducing the explicit expressions of $\mathbf{u}_{32}$ and $\mathbf{u}_{43}$ that formulas (22) provide, becomes

$$a_2\cos\theta_{41}+a_1\sin\theta_{41}+a_0=0 \tag{24}$$

where $a_0=\cos\alpha_4(\cos\theta_{21}\sin\alpha_2\sin\alpha_1+\cos\alpha_1\cos\alpha_2)-\cos\alpha_3$, $a_1=\sin\theta_{21}\sin\alpha_2\sin\alpha_4$, and $a_2=\sin\alpha_4(\cos\theta_{21}\sin\alpha_2\cos\alpha_1-\sin\alpha_1\cos\alpha_2)$.

Eq. (24) is transformable into a quadratic equation through the half-tangent substitution (i.e., the change of variable sinx=2t/(1 + t^2) and cosx=(1 − t^2)/(1 + t^2) where t=tan(x/2)) whose solution provides the following explicit expression of θ_{41} as a function of θ_{21}:

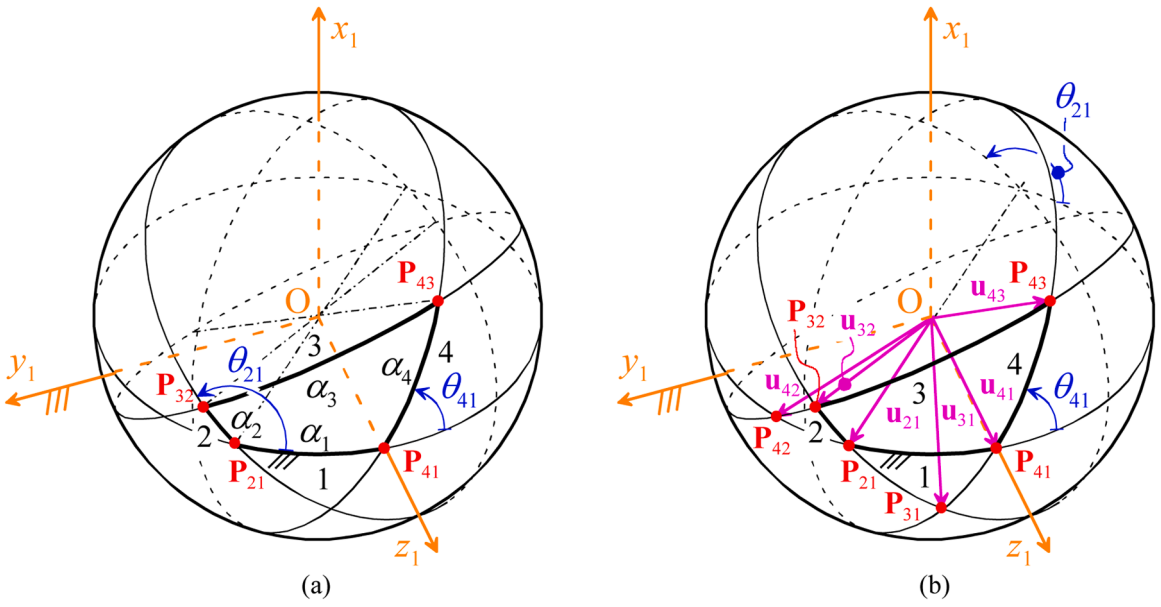

Fig. 5. Spherical four-bar linkage: (a) notations, (b) geometric determination of the IPAs.

$$\tan\left(\frac{\theta_{41}}{2}\right)=\frac{-a_1+(-1)^p\sqrt{a_1^2+a_2^2-a_0^2}}{a_0-a_2}\Rightarrow\theta_{41}=2\,\mathrm{atan2}\left(-a_1+(-1)^p\sqrt{a_1^2+a_2^2-a_0^2},\ a_0-a_2\right),\qquad p=0,1 \tag{25}$$

Moreover, Eq. (5) yields the following explicit expressions of the VCs ($\dot{q}=\dot{\theta}_{21}=\omega_{21}$):

$$\frac{\omega_{21}}{\dot{q}}=1;\qquad \frac{\omega_{31}}{\dot{q}}=\frac{\omega_{31}}{\omega_{21}}=\frac{(\mathbf{u}_{31}\times\mathbf{u}_{21})\cdot(\mathbf{u}_{32}\times\mathbf{u}_{21})}{(\mathbf{u}_{31}\times\mathbf{u}_{21})\cdot(\mathbf{u}_{32}\times\mathbf{u}_{31})} \tag{26a}$$

$$\frac{d\theta_{41}}{d\theta_{21}}=\frac{\dot{\theta}_{41}}{\dot{\theta}_{21}}=\frac{\omega_{41}}{\dot{q}}=\frac{\omega_{41}}{\omega_{21}}=\frac{(\mathbf{u}_{41}\times\mathbf{u}_{21})\cdot(\mathbf{u}_{42}\times\mathbf{u}_{21})}{(\mathbf{u}_{41}\times\mathbf{u}_{21})\cdot(\mathbf{u}_{42}\times\mathbf{u}_{41})} \tag{26b}$$

Eventually, Eq. (21) gives the following dynamic model of the spherical four-bar linkage

$$\begin{aligned}&\tau+Q_{2,p}+Q_3+Q_4=\ddot{\theta}_{21}\sum_{j=2,4}\left(\frac{\omega_{j1}}{\omega_{21}}\right)^2{}^1\mathbf{u}_{j1}^{T\,j}\mathbf{R}_1^{Tj}\mathbf{I}_{O\,j}{}^j\mathbf{R}_1{}^1\mathbf{u}_{j1}+\\&\quad+\frac{1}{2}\dot{\theta}_{21}^2\sum_{j=2,4}\left(\frac{\omega_{j1}}{\omega_{21}}\right)\left\{2{}^1\mathbf{u}_{j1}^{T\,j}\mathbf{R}_1^{Tj}\mathbf{I}_{O\,j}{}^j\mathbf{R}_1{}^1\mathbf{u}_{j1}\frac{d}{d\theta_{21}}\left(\frac{\omega_{j1}}{\omega_{21}}\right)+\right.\\&\quad\left.+\left(\frac{\omega_{j1}}{\omega_{21}}\right)\left[\frac{d\left({}^j\mathbf{R}_1{}^1\mathbf{u}_{j1}\right)}{d\theta_{21}}^T{}^j\mathbf{I}_{O\,j}{}^j\mathbf{R}_1{}^1\mathbf{u}_{j1}+{}^1\mathbf{u}_{j1}^{T\,j}\mathbf{R}_1^{Tj}\mathbf{I}_{O\,j}\frac{d\left({}^j\mathbf{R}_1{}^1\mathbf{u}_{j1}\right)}{d\theta_{21}}\right]\right\}\end{aligned} \tag{27}$$

where the VCs are expressed through formulas (26), the derivatives with respect to θ_{21} are computable by using formula (26b) as follows

$$\frac{d(\cdot)}{d\theta_{21}}=\frac{\partial(\cdot)}{\partial\theta_{41}}\frac{d\theta_{41}}{d\theta_{21}}+\frac{\partial(\cdot)}{\partial\theta_{21}}=\frac{(\mathbf{u}_{41}\times\mathbf{u}_{21})\cdot(\mathbf{u}_{42}\times\mathbf{u}_{21})}{(\mathbf{u}_{41}\times\mathbf{u}_{21})\cdot(\mathbf{u}_{42}\times\mathbf{u}_{41})}\frac{\partial(\cdot)}{\partial\theta_{41}}+\frac{\partial(\cdot)}{\partial\theta_{21}} \tag{28}$$

and

$$Q_{2,p}=\sum_{k=1,n_2}F_{2,k}\mathbf{u}_{21}\cdot\left[(A_{2,k}-O)\times\mathbf{v}_{2,k}\right]-\tau \tag{29a}$$

$$Q_3=\left(\frac{\omega_{31}}{\omega_{21}}\right)\sum_{k=1,n_3}F_{3,k}\mathbf{u}_{31}\cdot\left[(A_{3,k}-O)\times\mathbf{v}_{3,k}\right]=\frac{(\mathbf{u}_{31}\times\mathbf{u}_{21})\cdot(\mathbf{u}_{32}\times\mathbf{u}_{21})}{(\mathbf{u}_{31}\times\mathbf{u}_{21})\cdot(\mathbf{u}_{32}\times\mathbf{u}_{31})}\sum_{k=1,n_3}F_{3,k}\mathbf{u}_{31}\cdot\left[(A_{3,k}-O)\times\mathbf{v}_{3,k}\right] \tag{29b}$$

$$Q_4=\left(\frac{\omega_{41}}{\omega_{21}}\right)\sum_{k=1,n_4}F_{4,k}\mathbf{u}_{41}\cdot\left[(A_{4,k}-O)\times\mathbf{v}_{4,k}\right]=\frac{(\mathbf{u}_{41}\times\mathbf{u}_{21})\cdot(\mathbf{u}_{42}\times\mathbf{u}_{21})}{(\mathbf{u}_{41}\times\mathbf{u}_{21})\cdot(\mathbf{u}_{42}\times\mathbf{u}_{41})}\sum_{k=1,n_4}F_{4,k}\mathbf{u}_{41}\cdot\left[(A_{4,k}-O)\times\mathbf{v}_{4,k}\right] \tag{29c}$$

3.2. Numerical example of IP solution

In this subsection, a spherical four-bar linkage with the geometric data and the mass distribution data reported in Table 1 is considered and its IP is solved with the algorithms of Fig. 4 for the active-load data reported in Table 2.

3.2.1. Implementation of step (i)

In this case, the availability of explicit formulas for the position-analysis solution (i.e., Eq. (25)) and for all the IPA directions (i.e., Eqs. (22a), (22b), and (22e)) immediately makes this formulas the stored results of step (i). In practice, the algebraic manipulations

Table 1
Geometric data and inertia tensors of the links of the spherical four-bar linkage used in the numerical example.

j	α_j [rad]	${}^jI_{O,j}$ [kg m^2]
1	$\pi/3$	–
2	$\pi/9$	$\begin{bmatrix}2 & 0 & 0\\0 & 1.920725 & -0.335117\\0 & -0.335117 & 0.079275\end{bmatrix}$
3	$7\pi/18$	$\begin{bmatrix}7 & 0 & 0\\0 & 4.420725 & -2.529672\\0 & -2.529672 & 2.579275\end{bmatrix}$
4	$2\pi/9$	$\begin{bmatrix}4 & 0 & 0\\0 & 3.410633 & -1.183662\\0 & -1.183662 & 0.589367\end{bmatrix}$

Table 2
Active-load data used in the numerical example.

$Q_{2,p}$ [N m]	$Q_3/\left(\frac{\omega_{31}}{\omega_{21}}\right)$ [N m]	$Q_4/\left(\frac{\omega_{41}}{\omega_{21}}\right)$ [N m]
$-\sin\theta_{21}-2\dot{\theta}_{21}$	0	$-5\sin\theta_{41}-2\dot{\theta}_{41}$

that brought to those formulas replace the numerical solution of the closure equations for discretized values of q and the successive determination of the IPAs' directions for the same discretized values.

Fig. 6 shows the solutions of the position analysis, that is, the diagram of θ_{41} as a function of the generalized coordinate θ_{21} computed with Eq. (25).

3.2.2. *Implementation of step (ii)*

Here, firstly, the results of step (i) are used to compute the VCs and their first derivative with respect to θ_{21} (acceleration coefficients (ACs)) as a function of θ_{21} by using formulas (26) and (28), respectively. Successively, the computed VCs and ACs together with the mass distribution data of Table 1 and the active-load data of Table 2 are introduced into the built dynamic model (i.e., Eq. (27)) to compute the IP solution, that is, the generalized torque, τ, as a function of time, t, for the case $\theta_{21}=\omega_{21}\,t$, with ω_{21} constant and equal to 1 rad/s.

Figs. 7 and 8 show the diagrams of the VCs and the ACs, respectively, as a function of θ_{21} computed through formulas (26) and (28). In addition, Fig. 9 shows the diagram of the generalized torque, τ, as a function of time, t, (i.e., the IP solution) computed through Eq. (27).

3.3. *DP solution*

Regarding the DP solution, the numerical integration of Eq. (27) can be implemented in many ways (see [30] for details). For instance, in Eq. (27), the replacement of $\dot{\theta}_{21}$ and $\ddot{\theta}_{21}$ with their finite-difference approximations [30], that is, with the formulas (Δ is the finite increment of the discretized variable t)

$$\dot{\theta}_{21}(t_i)=\frac{\theta_{21}(t_i)-\theta_{21}(t_{i-1})}{\Delta},\qquad \ddot{\theta}_{21}(t_i)=\frac{\theta_{21}(t_{i+1})-2\,\theta_{21}(t_i)+\theta_{21}(t_{i-1})}{\Delta^2} \tag{30}$$

yields, after some rearrangement, the iterative formula

$$\theta_{21}(t_{i+1})=\frac{1}{g_1(\theta_{21}(t_i))}\left\{\Delta^2[Q_2(t_i)+Q_3(t_i)+Q_4(t_i)]-\frac{g_2(\theta_{21}(t_i))}{2}[\theta_{21}(t_i)-\theta_{21}(t_{i-1})]^2\right\}+2\,\theta_{21}(t_i)-\theta_{21}(t_{i-1}) \tag{31}$$

where

$$g_1(\theta_{21}(t_i))=\sum_{j=2,4}\left(\frac{\omega_{j1}}{\omega_{21}}\right)^2 {}^1\mathbf{u}_{j1}^T\,{}^j\mathbf{R}_1^{Tj}\,\mathbf{I}_{Oj}\,{}^j\mathbf{R}_1\,{}^1\mathbf{u}_{j1} \tag{32a}$$

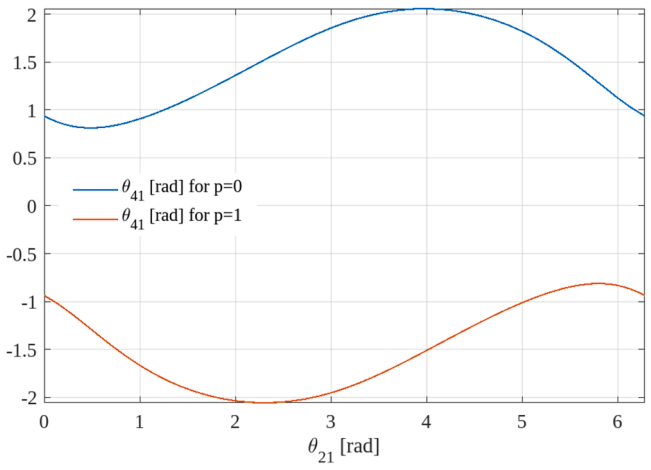

Fig. 6. Position-analysis solution (Eq. (25)) of the spherical four-bar linkage of Fig. 5 with the sizes reported in Table 1: diagram of joint variable θ_{41} as a function of the generalized coordinate θ_{21}.

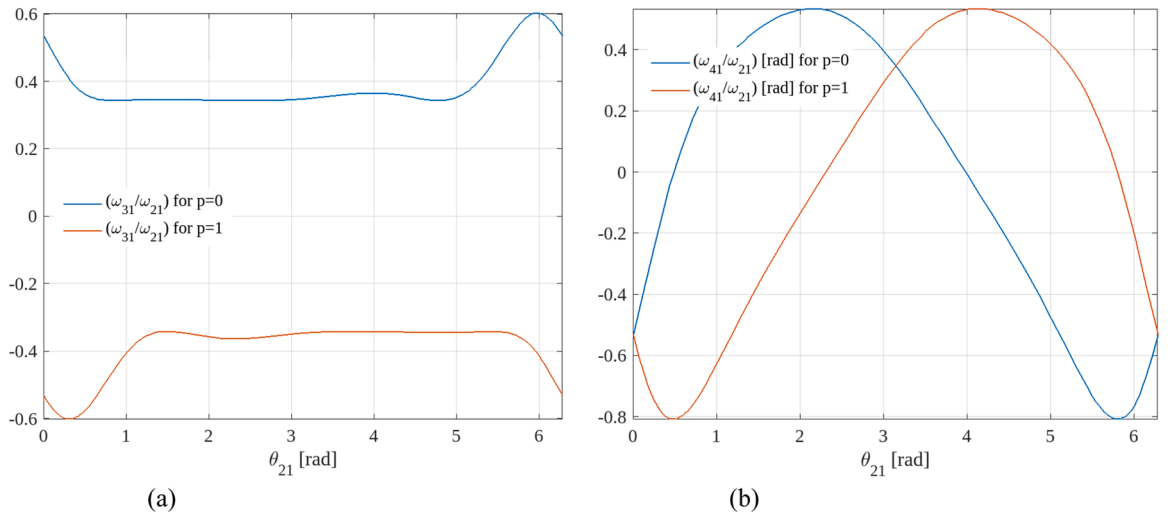

Fig. 7. Diagrams of the velocity coefficients (a) $(\omega_{31}/\omega_{21})$ (Eq. (26a)) and (b) $(\omega_{41}/\omega_{21})$ (Eq. (26b)) of the spherical four-bar linkage of Fig. 5, with the sizes reported in Table 1, as a function of the generalized coordinate $\theta_{21,}$ for the two possible solutions (Eq. (25)) of the position analysis.

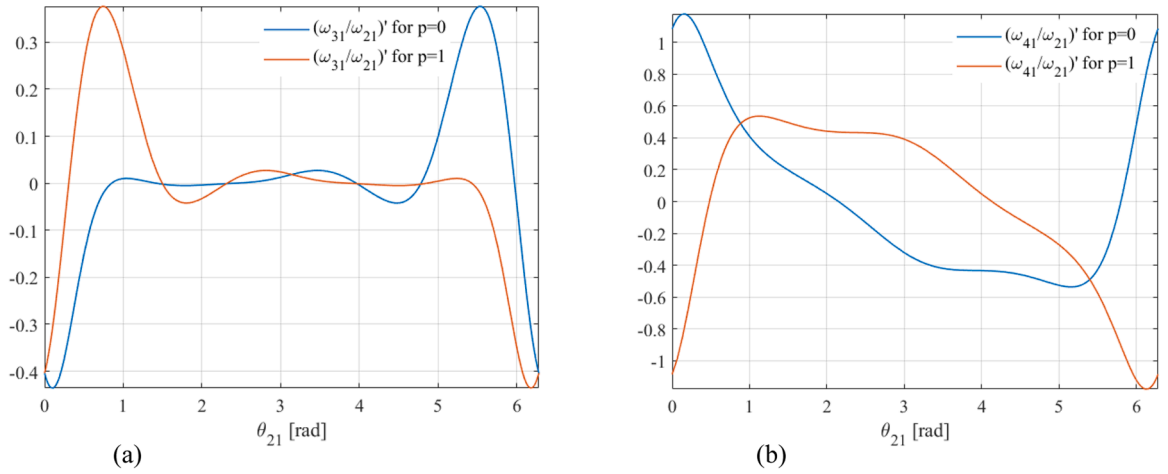

Fig. 8. Diagrams of the acceleration coefficients (a) $(\omega_{31}/\omega_{21})'$ and (b) $(\omega_{41}/\omega_{21})'$ of the spherical four-bar linkage of Fig. 5, with the sizes reported in Table 1, as a function of the generalized coordinate $\theta_{21,}$ for the two possible solutions (Eq. (25)) of the position analysis.

$$\left[g_2(\theta_{21}(t_i)) = \sum_{j=2,4} \left(\frac{\omega_{j1}}{\omega_{21}}\right) \left\{ 2\,{}^1\mathbf{u}_{j1}^{Tj}\,{}^j\mathbf{R}_1^{Tj}\,\mathbf{I}_{Oj}\,{}^j\mathbf{R}_1\,{}^1\mathbf{u}_{j1} \frac{d}{d\theta_{21}} \left(\frac{\omega_{j1}}{\omega_{21}}\right) + \right.\right.$$
$$\left.\left. + \left(\frac{\omega_{j1}}{\omega_{21}}\right) \left[\frac{d\left({}^j\mathbf{R}_1\,{}^1\mathbf{u}_{j1}\right)^T}{d\theta_{21}}\,{}^j\mathbf{I}_{Oj}\,{}^j\mathbf{R}_1\,{}^1\mathbf{u}_{j1} + {}^1\mathbf{u}_{j1}^{Tj}\,{}^j\mathbf{R}_1^{Tj}\,\mathbf{I}_{Oj} \frac{d\left({}^j\mathbf{R}_1\,{}^1\mathbf{u}_{j1}\right)}{d\theta_{21}} \right] \right\} \right. \tag{32b}$$

which, together with the initial conditions $\theta_{21}(t_0) = \theta_{21,0}$ and $\dot{\theta}_{21}(t_0) = \dot{\theta}_{21,0} (\Rightarrow \theta_{21}(t_1) = \dot{\theta}_{21,0}\,\Delta + \theta_{21,0})$, allows the numerical computation of the time history of the generalized coordinate (i.e., $\theta_{21}(t)$) when the time histories of all the active loads (i.e., $Q_2(t)$, $Q_3(t)$ and $Q_4(t)$) are known, that is, it allows the DP solution.

4. Discussion

The proposed procedure consists of two steps (see subSection 2.1.2), but, if the mechanism geometry does not change (as it is, for instance, in control algorithms), the 1st step and all the preliminary kinematic computations of the 2nd step, which are the ones that require the most burden of computation (in the case study of Section 3, all the diagrams of Figs. 6-8 are results of these computations and the same figures are an example on how these results could be stored), can be implemented only once and offline. As a consequence, the proposed procedure/model is fast enough to be used in demanding real-time control algorithms since they have to

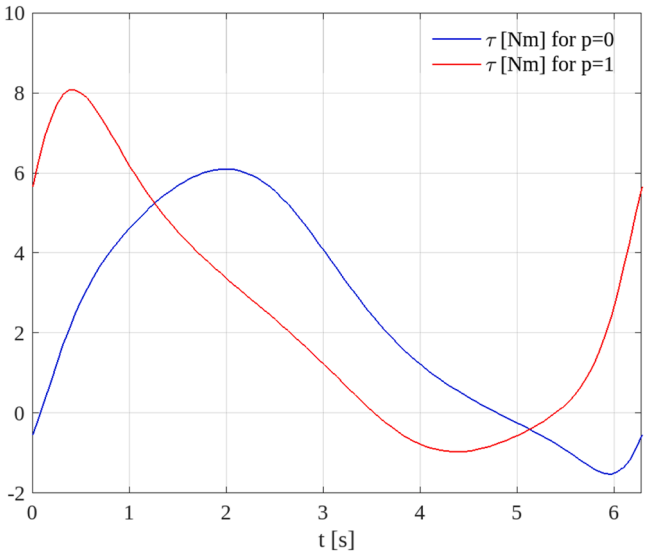

Fig. 9. Diagrams of the generalized torque τ as a function of time, *t*, computed through Eq. (27), for the case $\theta_{21}=\omega_{21}\,t$, with ω_{21} constant and equal to 1 rad/s, and the active-load data reported in Table 2, and for the two possible solutions (Eq. (25)) of the position analysis.

implement only the remaining computations of the 2nd step, which can retrieve the results of the offline computations from a database and, now, needs only the computation of one formula, Eq. (21), where all the terms uniquely depending on the generalized coordinate are retrieved from the database (in the above case study, Eq. (21) becomes Eq. (27) where all the terms appearing in the two summations are retrieved from the database). For instance, in the IP solution, the computation of the generalized torque, τ, with formula (21) uniquely requires the computation of the arithmetic operations appearing in that formula. The number of such arithmetic operations is of the same order of that of other lagrangian approaches or of well-structured Newton-Euler approaches and they can be implemented in real-time even with old microprocessors.

Moreover, the proposed model uses VCs, ACs and rotation matrices whose explicit expressions are in general easy to determine after the IPA directions have been expressed as functions of the generalized coordinate. Indeed, in the case study of Section 3, VCs and rotation matrices have been all immediately expressed as functions of IPA directions, which have been related to the mechanism configuration through the explicit formulas of the position-analysis solution; then, the ACs explicit expressions have been automatically deduced by differentiating the VCs with an algebraic manipulator (the "Symbolic Math Toolbox" of Matlab) without the need of really writing them in the program, where they appear as "functions". The same has been done for the other derivatives with respect to the generalized coordinate that appear in the model. It is worth stressing that formulas obtained from algebraic manipulators can always be displayed and copied into a different programming environment with a simple "cut and paste"; moreover, if an algebraic manipulator was not available, derivatives could always be numerically computed, for instance, through their finite-difference approximations [30].

In mechanism synthesis' problems, the computation burden is much less relevant than in real-time control applications since the mechanism design is an "offline" activity. Differently from real-time applications, implementing these problems through the proposed procedure requires the repetition of both the steps of the procedure every time some geometric constants are modified. Nevertheless, the fact that the proposed model directly relates the dynamic behavior of a mechanism to its geometry makes identifying the changes necessary to improve its dynamic performance easier, which is exactly what designers need to reduce design time when they have to match particular design requirements for the mechanism's dynamics.

In the literature, the dynamic models proposed for spherical mechanisms [17-20,31-37] use Newton-Euler formulation [19], Lagrangian formulation [31,33], and other formulations (Gibbs-Appell method [18], Virtual Work principle [35,36] even combined with Screw theory [37], etc.). Most of these approaches either focus on specific spherical architectures [17,19,32,33,36] or address specific issues (e.g., accuracy [20], control [35]). The few works devoted to general formulations [18,31,37] refer to multi-DOF spherical mechanisms and mainly adapt models conceived for spatial mechanisms to spherical ones thus losing the opportunity of taking advantage of single-DOF mechanisms' peculiarities when they are applied to single-DOF spherical mechanisms. Moreover, all the proposed approaches are mainly analytical even when they provide explicit formulas [18,31]. Differently, the dynamic model proposed here fully exploits the peculiarities of single-DOF spherical mechanisms and is deeply related to the mechanism configuration through the IPA directions thus providing a geometric interpretation of the terms appearing in it that facilitates the introduction of targeted changes in the mechanism geometry during the design process. Eventually, since Eksergian's equation [27] is deducible (see Appendix A) from the Lagrangian formulation of the 2nd kind, the approach proposed here is classifiable among those that use the Lagrangian formulation.

5. Conclusions

The fact that, in spherical single-DOF mechanisms, velocity coefficients (VCs) are expressible through instantaneous pole axes' (IPAs') directions and that Eksergian's equations provides a VC-based dynamic model, has allowed the deduction of a novel general dynamic model for single-DOF spherical mechanisms.

The proposed model fully exploits the peculiarities of single-DOF spherical mechanisms. In particular, the existence of exhaustive and fast algorithms that, in these mechanisms, analytically and geometrically relate the IPA directions to the mechanism configurations makes this model able to provide geometric interpretations of the terms appearing in it. Such interpretations relate the mechanism geometry to its dynamic behavior in a way that greatly facilitates the design process.

The algorithms that solve the inverse (IP) and the direct (DP) problems of mechanism dynamics by using the proposed model have been also presented. Such algorithms, when the mechanism geometry does not change, as it happens in real-time control, can be organized so that the most burden of computation is done once and offline. This feature makes the model usable even in demanding real-time applications.

Eventually, the effectiveness of the proposal has been also illustrated by applying it to a case study.

CRediT authorship contribution statement

Raffaele Di Gregorio: Writing – review & editing, Writing – original draft, Visualization, Validation, Supervision, Software, Resources, Project administration, Methodology, Investigation, Funding acquisition, Formal analysis, Data curation, Conceptualization.

Declaration of competing interest

The authors declare that they have no known competing financial interests or personal relationships that could have appeared to influence the work reported in this paper.

Data availability

No data was used for the research described in the article.

Acknowledgements

This work has been developed at the Laboratory of Mechatronics and Virtual Prototyping (LaMaViP) of Ferrara Technopole, supported by FIRD2023 UNIFE funds.

Appendix A

Eksergian's equation [24,26,27] can be deduced directly from Lagrange's equations of the 2nd kind since, in practice, it is the form that such equations assume in the case of single-DOF mechanical systems. Indeed, for a single-DOF system, Lagrange's equations of the 2nd kind become a unique equation that can be written as follows (q is the *generalized coordinate* of the single-DOF system))

$$\frac{d}{dt}\left(\frac{\partial E}{\partial \dot{q}}\right) - \frac{\partial E}{\partial q} = Q \tag{A.1}$$

where Q is the *generalized force* defined as follows (n is the number of active forces (including the conservative forces and excluding the inertial forces) applied to the system; $\mathbf{F}_r$ is the r-th active force, which is applied to point P_r; V is the *total potential energy* due to conservative forces; Q_{nc} is the contribution to Q due to non-conservative forces)

$$Q = Q_{nc} - \frac{dV}{dq} = \sum_{r=1,n} \mathbf{F}_r \cdot \frac{d\mathbf{P}_r}{dq} \tag{A.2}$$

and E is the *total kinetic energy*.

In a single-DOF system, E can be written as follows (M is the *total mass* of the system and B is the *equivalent moment of inertia*)

$$\left.\begin{aligned} E &= \frac{1}{2}\dot{q}^2 \int_M \frac{d\mathbf{P}}{dq} \cdot \frac{d\mathbf{P}}{dq} dM \\ B(q) &= \int_M \frac{d\mathbf{P}}{dq} \cdot \frac{d\mathbf{P}}{dq} dM \end{aligned}\right\} \Rightarrow E = \frac{1}{2}\dot{q}^2 B(q) \tag{A.3}$$

whose introduction into Eq. (A.1) yields

$$E = \frac{1}{2}\dot{q}^2 B(q) \Rightarrow \left.\begin{cases} \dfrac{\partial E}{\partial \dot{q}} = B(q)\dot{q} \Rightarrow \dfrac{d}{dt}\left(\dfrac{\partial E}{\partial \dot{q}}\right) = B(q)\ddot{q} + \dfrac{dB}{dq}\dot{q}^2 \\ \dfrac{\partial E}{\partial q} = \dfrac{1}{2}\dot{q}^2\dfrac{dB}{dq} \end{cases} \right\} \Rightarrow B(q)\ddot{q} + \frac{1}{2}\frac{dB}{dq}\dot{q}^2 = Q \qquad \text{(A.4)}$$

$$\frac{d}{dt}\left(\frac{\partial E}{\partial \dot{q}}\right) - \frac{\partial E}{\partial q} = Q$$

Equation (A.4) is Eksergian's equation in its general form.

References

[1] C.H. Chiang, Kinematics of Spherical Mechanisms, Krieger Publishing Company, Malabar, Florida, USA, 2000.
[2] T.A. Hess-Coelho, A redundant parallel spherical mechanism for robotic wrist applications, ASME J. Mech. Des. 129 (8) (August 2007) 891–895, https://doi.org/10.1115/1.2735645.
[3] M. Arredondo-Soto, E. Cuan-Urquizo, A. Gómez-Espinosa, A. Roman-Flores, P.D. Urbina-Coronado, M. Jimenez-Martinez, The compliant version of the 3-RRR spherical parallel mechanism known as "Agile-Eye": kinetostatic analysis and parasitic displacement evaluation, Mech. Mach. Theory 180 (2023) 105160, https://doi.org/10.1016/j.mechmachtheory.2022.105160.
[4] J.S. Navarro, N. Garcia, C. Perez, E. Fernandez, R. Saltaren, M. Almonacid, Kinematics of a robotic 3UPS1S spherical wrist designed for laparoscopic applications, Int. J. Med. Robotics Comput. Assist. Surg. 6 (2010) 291–300, https://doi.org/10.1002/rcs.331.
[5] N.M. Bajaj, A.J. Spiers, A.M. Dollar, State of the art in artificial wrists: a review of prosthetic and robotic wrist design, IEEE Trans. Rob. 35 (1) (February 2019) 261–277, https://doi.org/10.1109/TRO.2018.2865890.
[6] R.A.R.C. Gopura, K. Kiguchi, D.S.V. Bandara, A brief review on upper extremity robotic exoskeleton systems, in: 2011 6th International Conference on Industrial and Information Systems, Kandy, Sri Lanka, 2011, pp. 346–351, https://doi.org/10.1109/ICIINFS.2011.6038092.
[7] S. Mghames, M.G. Catalano, A. Bicchi, G. Grioli, A Spherical Active Joint for Humanoids and Humans, IEEE Robot. Autom. Lett. 4 (2) (April 2019) 838–845, https://doi.org/10.1109/LRA.2019.2893423.
[8] H. Fan, G. Wei, L. Ren, Prosthetic and robotic wrists comparing with the intelligently evolved human wrist: a review, Robotica 40 (11) (2022) 4169–4191, https://doi.org/10.1017/S0263574722000856.
[9] J.M. Hilkert, D.L. Amil, Structural effects and techniques in precision pointing and tracking systems: a tutorial overview, in: Proc. SPIE 7696, Automatic Target Recognition XX; Acquisition, Tracking, Pointing, and Laser Systems Technologies XXIV; and Optical Pattern Recognition XXI, 12 May 2010, p. 76961C, https://doi.org/10.1117/12.849836.
[10] J.M. Hervé, Uncoupled actuation of pan-tilt wrists, IEEE Trans. Rob. 22 (1) (Feb. 2006) 56–64, https://doi.org/10.1109/TRO.2005.858859.
[11 X. Kong, Forward displacement analysis of a 2-DOF RR-RRR-RRR spherical parallel manipulator, in: Procs. of 2010 IEEE/ASME International Conference on Mechatronic and Embedded Systems and Applications, Qingdao, China, 2010, pp. 446–451, https://doi.org/10.1109/MESA.2010.5551993.
[12] W. Li, J. Angeles, M. Valášek, Contributions to the kinematics of pointing, Mech. Mach. Theory 108 (2017) 97–109, https://doi.org/10.1016/j.mechmachtheory.2016.10.018.
[13] Q.J. Ge, P.M. Larochelle, Algebraic motion approximation with NURBS motions and its application to spherical mechanism synthesis, in: Procs. of the ASME 1998 Design Engineering Technical Conferences, Vol. 1B: 25th Biennial Mechanisms Conference, Atlanta, Georgia, USA, ASME, 1998, https://doi.org/10.1115/DETC98/MECH-5881. September 13–16V01BT01A009.
[14] J. Lenarcic, M. Stanisic, A humanoid shoulder complex and the humeral pointing kinematics, IEEE Trans. Robot. Autom. 19 (3) (June 2003) 499–506, https://doi.org/10.1109/TRA.2003.810578.
[15] X. Kong, C.M. Gosselin, A formula that produces a unique solution to the forward displacement analysis of a quadratic spherical parallel manipulator: the agile eye, ASME J. Mech. Robot. 2 (4) (November 2010) 044501, https://doi.org/10.1115/1.4002077.
[16] G. Mullineux, Atlas of spherical four-bar mechanisms, Mech. Mach. Theory 46 (11) (2011) 1811–1823, https://doi.org/10.1016/j.mechmachtheory.2011.06.001.
[17] E. Kayacan, Z.Y. Bayraktaroglu, W. Saeys, Modeling and control of a spherical rolling robot: a decoupled dynamics approach, Robotica 30 (4) (2012) 671–680, https://doi.org/10.1017/S0263574711000956.
[18] E. Abedloo, A. Molaei, H.D. Taghirad, Closed-form dynamic formulation of spherical parallel manipulators by Gibbs-Appell method, in: 2014 S RSI/ISM International Conference on Robotics and Mechatronics (ICRoM), Tehran, Iran, 2014, pp. 576–581, https://doi.org/10.1109/ICRoM.2014.6990964.
[19] A. Arian, B. Danaei, M.T. Masouleh, Kinematics and dynamics analysis of a 2-DOF spherical parallel robot, in: 2016 4th International Conference on Robotics and Mechatronics (ICROM), Tehran, Iran, 2016, pp. 154–159, https://doi.org/10.1109/ICRoM.2016.7886838.
[20] D.T. Vo, S. Kheylo, V.Q. Nguyen, Kinematic and dynamic accuracy of spherical mechanisms, Mech. Sci. 13 (2022) 23–30, https://doi.org/10.5194/ms-13-23-2022.
[21] R. Di Gregorio, Analytic and Geometric Technique for the Singularity Analysis of Multi-Degree-of-Freedom Spherical Mechanisms, ASME J. Mech. Robot. 7 (3) (2015) 031008, https://doi.org/10.1115/1.4028625, 9 pages.
[22] R. Di Gregorio, 2011, A general algorithm for analytically determining all the instantaneous pole axis locations in single-DOF spherical mechanisms, Proc. IMechE Part C: J. Mech. Eng. Sci. 225 (9) (2011) 2062–2075, https://doi.org/10.1177/0954406211404894.
[23] J.I. Valderrama-Rodríguez, J.M. Rico, J.J. Cervantes-Sánchez, A screw theory approach to compute instantaneous rotation axes of indeterminate spherical linkages, Mech. Based Des. Struct. Mach. 50 (8) (2022) 2836–2876, https://doi.org/10.1080/15397734.2020.1787841.
[24] S. Doughty, Mechanics of Machines, 2nd Ed., Doughty Samuel's profile on Academia.edu, Dubuque, IA, USA, 2019. Ver. 2.1 (edition self-produced by the author and freely downloadable from his profile).
[25] R. Di Gregorio, Analytical method for the singularity analysis and exhaustive enumeration of the singularity conditions in single-degree-of-freedom spherical mechanisms, in: Proc. IMechE Part C: J. Mechanical Engineering Science 227, 2013, pp. 1830–1840, https://doi.org/10.1177/0954406212469328.
[26] F. Wittenbauer, Graphische Dynamik, Springer-Verlag, Berlin, Germany, 1923.
[27] R. Eksergian, Ph.D. dissertation, 15 articles published on J. of the Franklin Institute, Voll. 209–211 (1930–1931), report an extended version of this thesis, Clark University, Worcester, MA, 1928.
[28] M.D. Ardema, Newton-Euler Dynamics, Springer, New York, NY, 2005.
[29] L.A. Pars, A Treatise On Analytical Dynamics, Heinemann, London, UK, 1965.
[30] C.-E. Fröberg, Introduction to Numerical Analysis, 2nd Ed., Addison-Wesley Publishing Company, Reading, Massachusetts (USA), 1969.
[31] R. Di Gregorio, V. Parenti-Castelli, Dynamics of a class of parallel wrists, ASME J. of Mech Des. 126 (3) (May 2004) 436–441, https://doi.org/10.1115/1.1737382.
[32] B. Danaei, A. Arian, M.T. Masouleh, A. Kalhor, Dynamic modeling and base inertial parameters determination of a 2-DOF spherical parallel mechanism, Multibody Sys.Dyn. 41 (4) (June 2017) 367–390, https://doi.org/10.1007/s11044-017-9578-3.

[33] X. Li, S. Bai, O. Madsen, Dynamic modeling and trajectory tracking control of an electromagnetic direct driven spherical motion generator, Rob. Comput. Integr. Manuf. 59 (2019) 201–212, https://doi.org/10.1016/j.rcim.2019.04.009.
[34] S. Bai, X. Li, J. Angeles, A review of spherical motion generation using either spherical parallel manipulators or spherical motors, Mech. Mach. Theory 140 (2019) 377–388, https://doi.org/10.1016/j.mechmachtheory.2019.06.012.
[35] A. Hassania, A. Bataleblua, S.A. Khalilpoura, H.D. Taghirada, P. Cardou, Dynamic Models of Spherical Parallel Robots for Model-Based Control Schemes, Cornell University, October 2021, https://doi.org/10.48550/arXiv.2110.00491. arXiv:2110.00491v1 [cs.RO].
[36] S. Staicu, Recursive modelling in dynamics of agile wrist spherical parallel robot, Rob. Comput. Integr. Manuf. 25 (2) (2009) 409–416, https://doi.org/10.1016/j.rcim.2008.02.001.
[37] J. Gallardo, J.M. Rico, A. Frisoli, D. Checcacci, M. Bergamasco, Dynamics of parallel manipulators by means of screw theory, Mech. Mach. Theory 38 (11) (2003) 1113–1131, https://doi.org/10.1016/S0094-114X(03)00054-5.